2013 European Control Conference (ECC)
July 17-19, 2013, Zürich, Switzerland.

Transformation-based Iterative Learning Control for Non-collocated Sensing of a Galvanometer Scanner

Han Woong Yoo[1,2], Shingo Ito[2], Michel Verhaegen[1], and Georg Schitter[2]

Abstract— **A transformation-based iterative learning control (ILC) approach is proposed to achieve accurate image scanning for the non-collocated dynamics of a galvanometer scanner. The non-collocation between the encoder and beam scanning mirror results in a tracking error of the actual beam position although the encoder measurement matches the reference signal. The proposed ILC is extended from the conventional ILC design by adding a reference transformation filter, which is based on the transfer functions between the measured and the controlled output. An error analysis shows that the proposed method can reduce the error of the actual controlled output, especially for applications of a large tracking reference such as image scanning. Experimental results with the proposed ILC show a better tracking accuracy as compared to conventional ILC design with non-collocated sensing.**

I. Introduction

Temporal resolution of confocal laser scanning microscopy has been improved for recording rapid biological processes such as a cardiac activity and the growth of intracellular structures [1]–[3]. To achieve the high temporal resolution, fast scanning devices such as a resonance scanner [4], a spinning disk [5], an acousto-optic deflector [6] have been applied. Changing the pinhole structure for a multiple illumination and detection has also been studied for fast imaging [2], [7]–[9].

In addition, there are approaches that improve control for fast confocal imaging with a conventional galvanometer based optical scanner. Galvanometer based optical scanners are most popular scanning systems for biological laser scanning confocal microscopes, which are usually provided as a default scanner [10], [11]. A modified bidirectional scanning function is studied for fast and undistorted imaging and applied to optical coherent tomography [12]–[14]. In a controller design of the galvanometer scanner, an indirect run to run (R2R) digital control has been studied for more accurate unidirectional, bidirectional, arbitrary scanning functions [15], [16]. Iterative learning control (ILC) is proposed for fast and accurate scanning confocal microscopy [17]. Due to non-collocation between the galvanometer scanner's encoder sensor and the actual scanning mirror, however, the beam position corresponding to the scanning mirror shows a distinct mismatch from the encoder sensor output at a high frequency, which results in image distortion in high speed microscope imaging with a galvanometer scanner. For measuring the actual beam position, an additional sensor requires not only cost and space, but a beam sampler is also not suitable for biological confocal fluorescence microscopy, because of the limited number of photons in fluorescence imaging and the risk of photobleaching when increasing the laser power for a better image contrast.

In this paper, a transformation-based iterative learning control is proposed to compensate for the non-collocated sensing when applying iterative learning control. Non-collocation between the desired and the measured output has been studied by an observer-based structure in [18], [19] and applied to a robot control. Their method estimates the controlled output from the measured output by applying the transfer function between these two outputs, and their tracking error performance is intensively analysed. Instead of filtering the output or adding an observer, the proposed method modifies the reference signal to the desired measured output reference based on the internal model theorem [20]. This approach is simple in design, as the ILC and the reference transformation filter can be designed separately, even though the convergence criterion is still the same with conventional ILC. The proposed method is also computationally efficient since the reference transformation can be done once and in advance for a given reference. The final error with a bounded measurement uncertainty is analysed. Experimental results with a commercial galvanometer scanner demonstrate the benefits of the proposed ILC, and is compared to the conventional ILC based on both the measured and controlled output directly.

This paper is organised as follows. Section II introduces the non-collocation problem of a galvanometer scanner with its frequency analysis. Section III describes the proposed transformation-based ILC design with an error analysis for the beam position output. In Section IV, experimental results demonstrate the benefits of the proposed ILC. The conclusion is given in Section V.

II. Non-collocated Dynamics of Galvanomter Scanner

Fig. 1 shows a mechanical model of a moving-magnet galvanometer scanner, which is typically used in confocal laser scanning microscopy [10], [11]. A scanning mirror is attached at one end of the shaft for beam positioning. At the other end, an encoder is placed for the measurement of the deflection angle. The magnets with the encoder and the

This research was supported by the Integrated Smart Microscopy project in the Smart Optics Systems program of the Technologiestichting STW, the Netherlands, and by an Ernst-Mach-Stipendium of the Austrian Agency for International Cooperation in Education & Research (OeAD).

[1]H. W. Yoo and M. Verhaegen are with Delft Center for Systems and Control, Delft University of Technology, Mekelweg 2, 2628 CD Delft, the Netherlands. {h.w.yoo, m.verhaegen}@tudelft.nl

[2]H. W. Yoo, S. Ito, and G. Schitter are with Automation and Control Institute, Vienna University of Technology, Gusshausstrasse 27-29, 1040 Vienna, Austria {ito, schitter}@acin.tuwien.ac.at

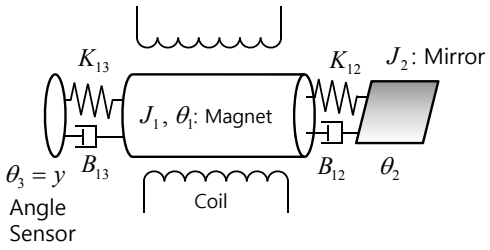

Fig. 1. A mechanical model of a moving magnet galvanometer scanner. The rotor of a galvanometer scanner consists of a magnet, a mirror and an encoder connected by the shaft. This shaft can be regarded as a spring (K_{12} and K_{13}) with damping (B_{12} and B_{13}) causing non-collocation between the encoder and the mirror.

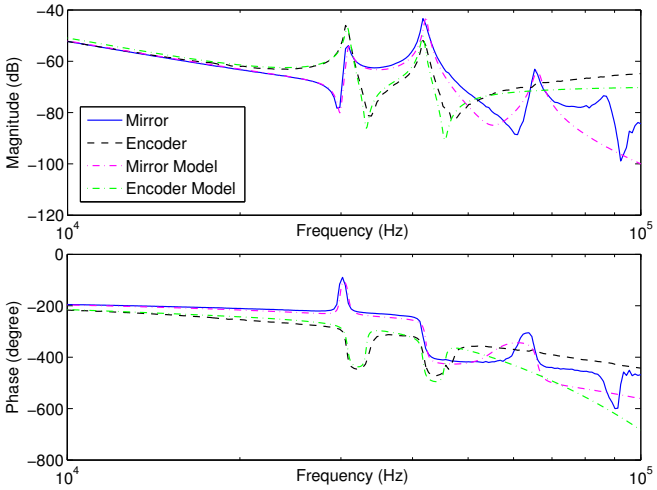

Fig. 2. Bode plot of the encoder and mirror position of the closed loop galvanometer with respect to the galvanometer input. The position of the anti-resonances varies for the two different outputs, which shows that the mirror position is not collocated with the encoder. The DC offset of the mirror position is adjusted. The fitted model for each output is discussed in Section IV.

mirror are rotated by the Lorentz force exerted by the current through the surrounded fixed coils.

Fig. 2 illustrates measured Bode plots of the encoder output and mirror position of the stabilised galvanometer scanner, measured by a Dynamic Signal Analyzer (HP3562, Agilent Technologies, Santa Clara, CA, USA) using a swept-sine signal as an input. At a low frequency, the shaft is stiff enough and both output signals follow the mass line of the total mass. At high frequencies, however, the encoder and the scanning mirror are decoupled due to limited stiffness of the shaft as shown in Fig. 1. This can be explained by a combination of multi-body dynamical systems [21]. This decoupling results in resonance and anti-resonances, which are different for each mass. The Bode plots show that the encoder and the scanning mirror angle are not collocated, which is evident by the different responses at high frequency beyond 20 kHz. Especially the anti-resonance at 33 kHz appears only in the Bode plot for the mirror output and is the clear evidence of this decoupling. The phase of the frequency response shows a time delay in the encoder output, which is assumed to be due to the electronics of the optical encoder.

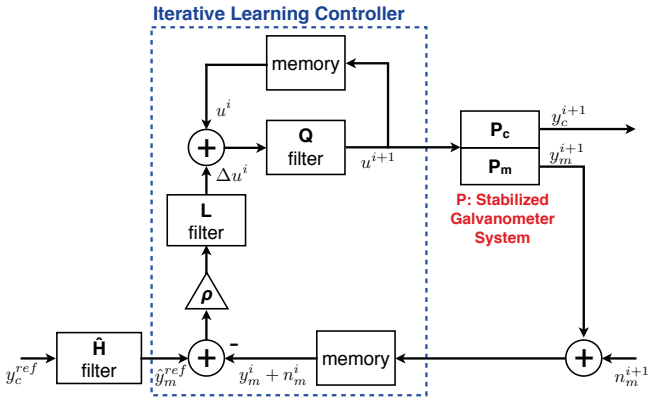

Fig. 3. A structure of transform-based iterative learning control with non-conllocated sensing. The stabilized galvanometer scanning system has two outputs, a measured output from an encoder and a controlled output from an actual beam position. The difference in dynamics are represented by each transfer functions, P_m, P_c. The reference transformation filter $\hat{H}$ is applied to achieve the desired reference of controlled output y_c^{ref} using an ILC with measured output.

Since the positions of poles are not affected by the non-collocated sensing, all poles of both outputs are expected to have the same frequency and damping.

This non-collocated sensing from the output that actually should be controlled causes an uncompensated error by ILC which limits its tracking performance. A transformation-based ILC is proposed in the following section, given with an error analysis.

III. Transformation-based Iterative Learning Control for Non-collocated Sensing

Fig. 3 shows the structure of the transformation-based iterative learning control with a stabilised galvanometer scanner [17], [22]. The structure leads to the following equations

$$u^{i+1}[k] = Q(q)\left(u^i[k] + \rho L(q)\left(e_m^i[k] - n_m^i[k]\right)\right), \quad (1)$$
$$e_m^i[k] = \hat{y}_m^{ref}[k] - y_m^i[k], \quad (2)$$
$$e_c^i[k] = y_c^{ref}[k] - y_c^i[k], \quad (3)$$
$$y_m^i[k] = P_m(q)u^i[k], \quad (4)$$
$$y_c^i[k] = P_c(q)u^i[k], \quad (5)$$

where $u^i[k]$, $y_c^i[k]$, $y_m^i[k]$, $e_c^i[k]$ and $e_m^i[k]$ denote the ILC input, controlled output, measured output, tracking error of the beam position, and measured tracking error of the encoder signal at the discrete time k in the ith trial. $\rho L(q)$, $Q(q)$, and $P_m(q)$ denote the LTI dynamics of the learning filter with a scalar learning gain ρ, the Q-filter, and the dynamics of the galvanometer scanner with the forward time-shift operator q, i.e. $x[k+1] = qx[k]$. $\hat{y}_m^{ref}$ and y_c^{ref} are the desired reference trajectories for the measured output and controlled output, respectively. $n_m^i[k]$ is a measurement noise at the measured output. It is assumed that the magnitude of the measurement noise at any frequency w and any iteration i is bounded by an arbitrary function δ, i.e. $|n_m^i(w)| < \delta(w), \forall w$ and $\forall i$ [23]. The design of the learning filter $L(q)$ of a minimum phase SISO plant dynamics is simply obtained by the inversion of the system, which is called an inversion

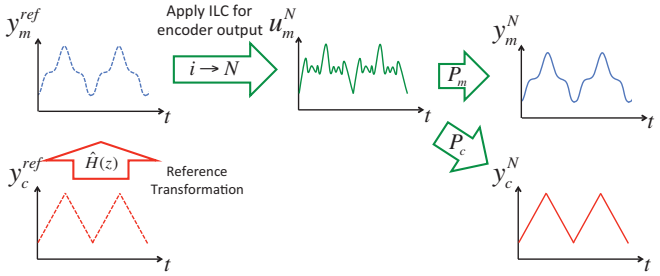

Fig. 4. A concept of the transformation-based ILC. The reference is modified based on the reference transformation filter $\hat{H}$ and applied to the ILC with the measured output. If the ILC reaches the final iteration N that ILC does not reduce the tracking error anymore by iteration, the controlled output also converges to the desired refernce by the non-collocation between two systems of the measured and controlled output.

based ILC. The Q filter is designed to cut off the learning at a certain frequency considering the convergence of ILC [24].

The goal of the transformation-based ILC is to minimise the tracking error of the beam position output via controlling the encoder measurement output by designing a reference transformation filter $\hat{H}(q)$, i.e.

$$\hat{y}_m^{ref}[k] = \hat{H}(q) y_c^{ref}[k]. \quad (6)$$

Fig. 4 illustrates the concept of the transformation-based ILC. Based on the desired trajectory for the laser beam, the reference transformation filter generates a new reference for the encoder measured output. Once the ILC designed for the measured output converges to the transformed reference, the output representing the beam position follows the actual desired reference y_c^{ref}. The boundedness of the final error of the ILC and of the bounded measurement noise is studied in Lemma 1 of [23]. Based on that, the following lemma provides the bounded final error of the proposed method.

Lemma 1: The limit of residual controlled output error is bounded by the following affine function of the reference function $y_c^{ref}(jw)$ and the noise effect $\delta(w)$,

$$\begin{aligned} |e_c^{\infty}(jw)| &= \lim_{i\to\infty} |e_c^i(jw)| \\ &\le \left(\left| H^{-1}(jw)\hat{H}(jw)\frac{1-Q(jw)}{1-\Phi(jw)} \right| \right. \\ &+ \left. \left| 1 - H^{-1}(jw)\hat{H}(jw) \right| \right) |y_c^{ref}(jw)| \\ &+ \left| H^{-1}(jw)\frac{P_m(jw)Q(jw)L(jw)}{1-\Phi(jw)} \right| \delta(w), \quad (7) \\ H(jw) &= P_m(jw)P_c^{-1}(jw), \quad (8) \end{aligned}$$

provided that the ILC with the measured output converges, i.e.

$$\Phi(jw) = Q(jw)(1-\rho P_m(jw)L(jw)) < 1, \forall w. \quad (9)$$

Proof: From (2), (4) and (1), the measured error dynamics along iteration axis is given as follows.

$$\begin{aligned} e_m^{i+1}[k] &= Q(q)(1-\rho P_m(q)L(q))e_m^i[k] \\ &+ \hat{H}(q)(1-Q(q))y_c^{ref}[k] \\ &+ \rho P_m(q)Q(q)L(q)n_m^i[k], \quad (10) \end{aligned}$$

(8) can be rewritten by $y_c^i = H^{-1}y_m^i$ from (4) and (5). Based on this, the controlled tracking error (3) can be rewritten by the measured tracking error (2) regarding the transformed reference (6) as

$$\begin{aligned} e_c^i[k] &= H^{-1}(q)e_m^i[k] \\ &+ \left(1 - H^{-1}(q)\hat{H}(q)\right) y_c^{ref}[k]. \quad (11) \end{aligned}$$

Assuming that the ILC converges, the final controlled tracking error in the frequency domain can be bounded as follows [23].

$$\begin{aligned} \lim_{i\to\infty} e_m^i(jw) &\le \hat{H}(jw)\frac{1-Q(jw)}{1-\Phi(jw)} y_c^{ref}(jw) \\ &+ \frac{P_m(jw)Q(jw)L(jw)}{1-\Phi(jw)}\delta(w). \quad (12) \end{aligned}$$

Substituting (12) with (11), the final controlled output error is obtained,

$$\begin{aligned} \lim_{i\to\infty} e_c^i(jw) &\le H^{-1}(jw)\hat{H}(jw)\frac{1-Q(jw)}{1-\Phi(jw)} y_c^{ref}(jw) \\ &+ \left(1 - H^{-1}(jw)\hat{H}(jw)\right) y_c^{ref}(jw) \\ &+ H^{-1}(jw)\frac{P_m(jw)Q(jw)L(jw)}{1-\Phi(jw)}\delta(w). \quad (13) \end{aligned}$$

By triangular inequality, (7) is obtained from (13). ■

Remark 1: Assuming that the desired controlled output reference and the complement of Q filter are orthogonal by design, i.e. $(1 - Q(jw)) y_c^{ref}(jw) = 0, \forall w$, the design of $\hat{H}(jw)$ is simply obtained by $H(jw)$.

Corollary 1: The final tracking error of the non-collocated system with a conventional ILC is obtained by applying $\hat{H}(jw) = 1$. Assuming an ideal case that a best design of the ILC is given with the perfect knowledge of the system $P_m(jw)$, the reference being designed to be orthogonal to the Q filter and $\hat{H} = H$, and zero noise $n_m^i[k] = 0$, $\forall i$ and $\forall k$, the error by non-collocation sensing is rewritten as follows:

$$|e_c^*(jw)| \le |e_m^*(jw)| + |1 - H^{-1}(jw)||y_c^{ref}(jw)|, \quad (14)$$

where e_c^* and e_m^* denote the optimal tracking errors of the controlled output and measured output. This corresponds to the results presented in [18].

Remark 2: Since $H(jw)$ represents the difference in dynamics between the measured output and the controlled output, in conventional ILC whose measured output equals to the controlled output, (8) degenerates $H(jw) = 1$. With $\hat{H}(jw) = 1$, this cancels the second term in (7), i.e. $1 - H^{-1}(jw)\hat{H}(jw) = 0$, which leads to (5) in [23].

Corollary 1 shows that the reference transformation filter can provide a smaller error than conventional ILC when the filter is designed appropriately. Moreover, it also implies that the error of non-collocated sensing depends on not only the mismatch by non-collocation between measured and controlled output but also on the tracking reference. This means that the proposed reference transformation filter is more beneficial with a large varying tracking reference such as an imaging scanning application.

In implementation, the proposed reference transformation methods is beneficial because of the simplicity of the design, without online computation for a given reference. The ILC can be designed and verified separately with the reference transformation filter, reducing the design effort and complexity. In addition, the computation of the transformation is only necessary when the reference changes. The following section presents experimental results for a fast and accurate beam scanning application with a high performance galvanometer scanner.

IV. Experimental Results

The transformation-based ILC is examined for a high performance galvanometer scanner (6210H, Cambridge Technology Inc., Lexington, MA, USA), which is a moving magnet type. Aforementioned, the encoder and actual mirror position, which is measured by the beam position, are non-collocated and show different dynamics. To illustrate the benefits of the transformation based ILC (ILC-PSDEst), a conventional ILC based on the encoder output without reference transformation (ILC-ENC) and based on the directly measured beam position output (ILC-PSD) are examined for comparison.

A. Experimental Setup

A high performance galvanometer scanner (6210H, Cambridge Technology Inc., Lexington, MA, USA) with a mirror for a laser beam diameter of $3mm$ is used, which is applied as laser scanning system in commercial laser confocal microscopes [10]. As shown in Fig. 5a, the galvanometer is driven by a servo driver (MicroMax 671, Cambridge Tech). The server driver applies the total input u^{tot} as a coil current, which is the summation of the ILC signal u^i and the output of the analog tamed PD controller u^{fb}.

Fig. 5b shows a beam scanning system to measure the mirror angle of the galvanometer, θ_2, directly. A red laser is emitted from a laser diode and passes through the pinhole (25 μm, Edmund optics) with collimating lenses L1 (Aspheric Lens, f = 11 mm, Thorlabs) and L2 (plano convex lens, f = 40 mm, Thorlabs). Then the beam is reflected by the scanning mirror and collimated to a position sensitive detector (PSD, S3932, Hamamatsu Photonics K.K., Hamamatsu, Japan) by the lens L3 (Plastic Aspheric, f =17.50 mm, Edmund optics).

Both encoder output and PSD output are sampled with $f_s = 526$ kHz, $T_s = 1.9$ μs by a data acquisition card (DAQ-2010, ADLink Technology Inc., New Taipei City, Taiwan). The measurements are processed in Labview (National Instruments Co., Austin, TX, USA) that manages the seamless streaming of the scanning signal while calculating the updated scanning signal via ILC in Matlab. A 2.06 kHz FIR-filtered triangular signal with a scanning amplitude for an optical angle of $0.190°$ is used as a reference y^{ref} [17].

B. System Modeling and Inversion-based ILC Design

For design of an inversion based ILC, the plant models of encoder output P_{enc} and PSD output P_{psd} are necessary. From the measured Bode plots shown in Fig. 2, the models

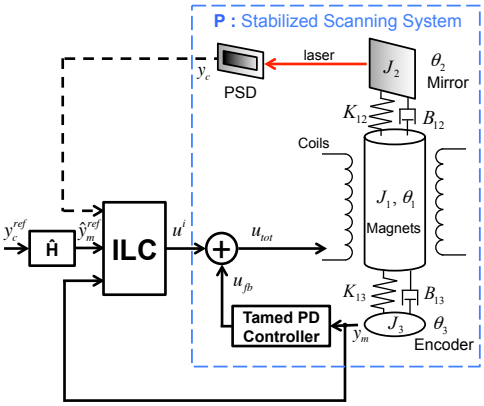

(a) Overall System

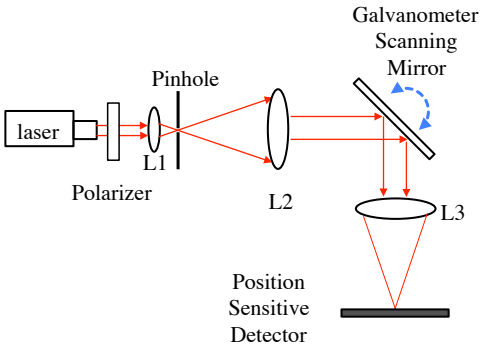

(b) Optical System

Fig. 5. (a) A diagram of the overall system with a PD stabilized scanning system. The marginally stable galvanometer scanner is stabilized by a tamed PD controller which regulates the galvanometer at less than 1kHz. ILC is applied to the feedback stablized galvanometer scanner up to a bandwith of 42 kHz, i.e. far beyond the feedback bandwidth. The reference transformation filter $\hat{H}$ is applied to the desired reference of the controlled output y_c^{ref}. (b) Schematic of a beam scanning system to measure the mirror angle (θ_2) directly. The beam is filtered by a pinhole and expanded by the lenses L1 and L2 before and after the the pinhole . The mirror angle is projected onto a lateral beam position at the position sensitive detector (PSD) by the lens L3.

are obtained by manually fitting multiple second order systems with a time delay. For example, the transfer function from the system input, given by the current through the coils of the galvanometer, to the encoder output P_{enc} is given as follows [17].

$$P_{enc}(s) = \frac{K \prod_{i_z=1}^{n_z} (s^2 + 2\zeta_{i_z}\omega_{i_z}s + \omega_{i_z}^2)}{\prod_{i_p=1}^{n_p} (s^2 + 2\zeta_{i_p}\omega_{i_p}s + \omega_{i_p}^2)} e^{-t_d \times 10^{-6} s}, \tag{15}$$

where K denotes a gain, t_d is a time delay in μs. n_p and n_z denotes the number of poles and zero, respectively. The transfer function from the same input to the actual position of the laser beam P_{psd} is represented in the same way with different parameters. Table I provides all parameters for each transfer function, and their Bode plot are shown by the magenta and the green dashed-dot line in Fig. 2.

The learning filter L is designed by inverting the respective model. The learning filter of L_{enc} of ILC-ENC and ILC-

TABLE I

PARAMETERS OF THE GALVANOMETER SCANNER OUTPUT MODELS

	Poles		Zeros		t_d	K
	$\omega/2\pi$	ζ	$\omega/2\pi$	ζ		
P_{ENC}	280	0.65	25000	0.6	18.5	3.32×10^{-4}
	30800	0.0087	33200	0.0069		
	41700	0.008	45500	0.0084		
P_{PSD}	250	0.65	29900	0.0069	5.5	2.81×10^{18}
	30900	0.0087	55000	0.07		
	42200	0.008				
	66000	0.015				

TABLE II

THE FINAL RMS ERRORS OF ILC-ENC, ILC-PSD, AND ILC-PSDEST

	ILC-ENC	ILC-PSD	ILC-PSDEst
RMS Error [10^{-3} °]	5.193	0.416	0.686

PSDEst is obtained by the inversion of P_{enc} [17]. The learning filter of ILC-PSD, L_{psd} is the inversion of the beam position model, P_{psd}^{-1}. For designing the Q-filter, a zero-phase 8th order Butterworth IIR filter with a bandwidth of 42kHz is used in all case, which is the position of the second resonance shown in Fig. 2. The learning gains of ILC-ENC, ILC-PSD, and ILC-PSDEst are set as 1, 0.2, and 0.5 respectively, considering the convergence of each ILC. The final trajectory is chosen where the ILC cannot improve the tracking performance anymore. The final iteration is chosen at the 30th iteration in ILC-ENC and ILC-PSDEst. For ILC-PSD, the 60th iteration is chosen, considering the slower convergence due to the smaller learning gain. The reference transformation filter is designed by dividing two models, i.e. $\hat{H} = P_{enc}/P_{psd}$.

C. Tracking Results

Fig. 6 shows the tracking result of ILC-ENC (magenta dashed line), ILC-PSD (blue dash-dot line), and ILC-PSDEst (black solid line) at the final iteration. The final root mean square (RMS) tracking error of each ILC is summarised in Table II. Not only ILC-PSD but also ILC-PSDEst in Fig. 6a tracks without phase-lag while ILC-ENC has a constant lag which is mainly due the the time delay of the encoder sensor output discussed in Section II. Fig. 6b and Table II shows that ILC-PSDEst results in a 7.5 times smaller tracking error than ILC-ENC. However, the tracking error is still 1.65 times larger than ILC-PSD. This is expected because ILC-PSD exploits full information of the desired output of the laser beam position, while ILC-PSDEst does not. ILC-PSDEst is still practically advantageous considering the fact that this beam position output is not available during operation of the confocal microscope. The control signal obtained via ILC also show that the input of ILC-PSDEst is more similar with ILC-PSD than ILC-ENC. The proposed ILC-PSD and its alternative solution ILC-PSDEst for the galvanometer scanner is beneficial for a fast and accurate imaging of scanning microscopes providing high temporal resolution and distortion free imaging.

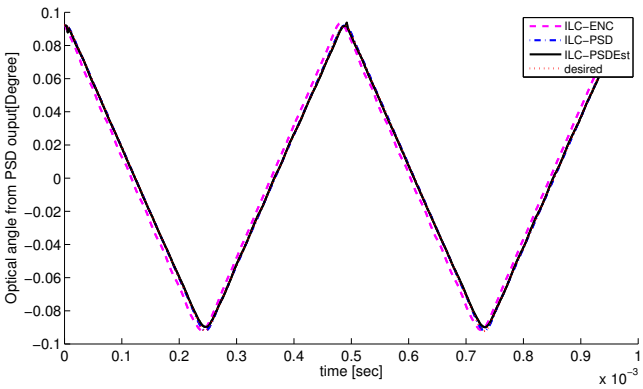

(a) Beam position trajectory

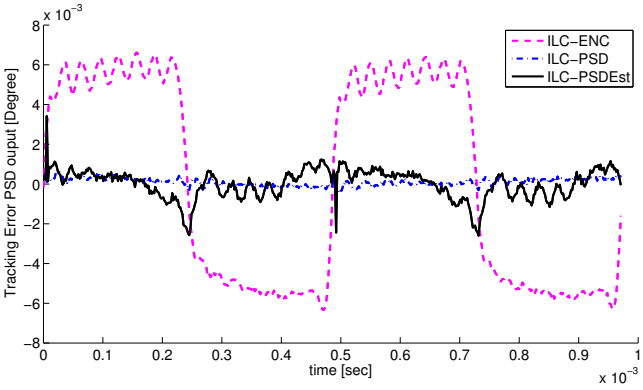

(b) Beam position error trajectory

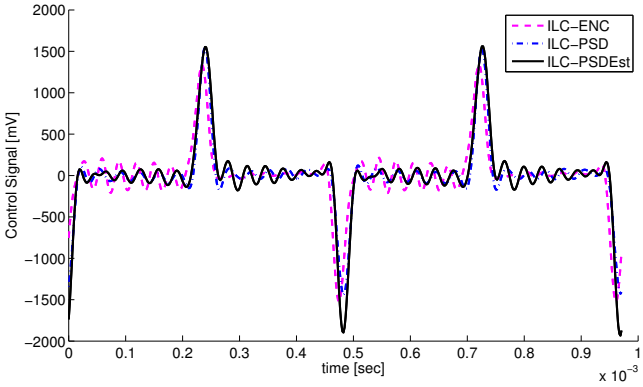

(c) Input Trajectory

Fig. 6. Final trajectories of ILC – PSDEst (black solid line), ILC – PSD (blue dash-dot line), and ILC – ENC (magenta dashed line) at a 2.06kHz scanning frequency.

V. CONCLUSION

In this paper, a transformation-based iterative learning control approach is proposed for non-collocated sensing of a galvanometer scanner. The dynamic mismatch introduced by the non-collocation of the galvanometer scanner's outputs is addressed as a bottleneck of iterative learning control design. An analysis of multi-body dynamics of the galvanometer scanner is given based on the measured Bode plots. The proposed transformation-based iterative learning control improves the tracking performance of the beam position output using the measured encoder output, by transforming

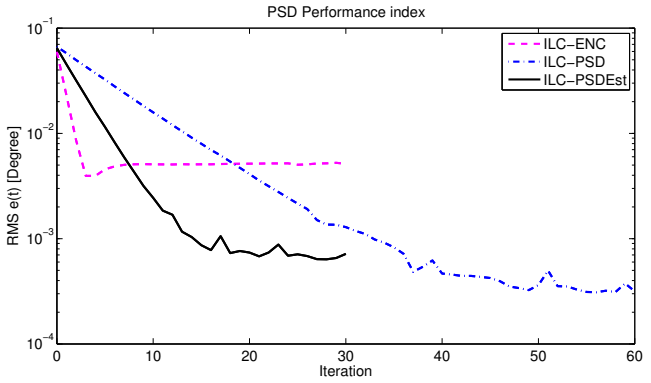

Fig. 7. RMS beam position error along ILC iterations. The variation in the convergence speed is due to different learning gains, depending on the stability conditions for the various ILC inputs.

the desired scanning reference. The upper bound of the final tracking error is analysed, and the desired transformation filter is driven derived under the assumption of zero output noise. Experimental results show that the proposed transformation-based ILC, ILC-PSDEst, reduces the tracking error up to 7.5 times as compared to ILC based directly on the encoder output, ILC-ENC, and is only 1.65 times larger than ILC with the directly measured laser beam position, which is used only for this evaluation but is not available when operating the confocal microscope. This proposed ILC is suitable for fast and distortion-free imaging in scanning confocal microscopy.

Current work is focused on a robust design of the reference transformation filter to reduce the unwanted oscillation in control and output signals, and evaluate it with a galvanometer scanner for the reliable laser scanning. A mechanical analysis and design of the galvanometer scanner is also investigated for the non-collocation problem of the sensor.

REFERENCES

[1] P. Saggau, "New methods and uses for fast optical scanning," *Current Opinion Neurobiology*, vol. 16, pp. 543–550, 2006.

[2] A. P. Baader, L. Buchler, L. Bircher-Lehmann, and A. G. Kleber, "Real time, confocal imaging of Ca2+ waves in arterially perfused rat hearts," *Cardiovasc Res.*, vol. 53, no. 1, pp. 105–115, 2002.

[3] E. Meijering, I. Smal, and G. Danuser, "Tracking in molecular bioimaging," *IEEE Signal Processing Magazine*, vol. 23, no. 3, pp. 46–53, 2006.

[4] N. Callamaras and I. Parker, "Construction of a confocal microscope for real-time x-y and x-z imaging," *Cell Calcium*, vol. 26, no. 6, pp. 271–279, 1999.

[5] M. D. Egger and M. Petran, "New reflected-light microscope for viewing unstained brain and ganglion cells," *Science*, vol. 157, pp. 305–307, 1967.

[6] S. R. Goldstein, T. Hubin, and S. Rosenthal, "A confocal video-rate laserbeam scanning reflected-light microscope with no moving parts," *J. Microscope*, vol. 127, pp. 29–38, 1990.

[7] A. Ichihara, T. Tanaami, K. Isozaki, Y. Sugiyama, and Y. Kosugi, "High-speed confocal fluorescence microscopy using a nipkow scanner with microlenses for 3d imaging of single fluorescence molecule in real time," *Bioimages*, vol. 4, pp. 57–62, 1996.

[8] T. Tanaami, S. Otsuki, N. Tomosada, Y. Kosugi, M. Shimizu, and H. Ishida, "High-speed 1-frame/ms scanning confocal microscope with a microlens and nipkow disks," *Applied Optics*, vol. 41, pp. 4704–4708, 2002.

[9] F. P. Martial and N. A. Hartell, "Progammable illumination and high-speed, multi-wavelength, confocal microscopy using digital micromirror," *PLOS ONE*, vol. 7, no. 8, p. e43942, 2012.

[10] J. B. Pawley, Ed., *Handbook of biological confocal microscopy*, 3rd ed. Springer Science Business Media, 2006.

[11] R. P. Aylward, "Advanced galvanometer-based optical scanner," *Sensor review*, vol. 23, no. 3, p. 2160222, 2003.

[12] V.-F. Duma, A. G. Podoleanu, and M. Nicolov, "Modeling a galvanoscanner with an optimized scanning function," *SYROM*, pp. 539–548, 2009.

[13] V.-F. Duma, "Mathematical functions of a 2-d scanner with oscilating elements," *Modeling, Simulation and Control of Nonlinear Engineering Dynamical Systems*, pp. 243–253, 2009.

[14] V.-F. Duma, K.-S. Lee, P. Meemon, and J. P. Rolland, "Experimental investigation of the scanning functions of galvanometer-based scanners with applications in oct," *Applied Optics*, vol. 50, no. 29, pp. 5735–5749, 2011.

[15] O. Trepte and A. Liljeborg, "Computer control for a galvanometer scanner in a confocal scanning laser microscope," *Optical Engineering*, vol. 33, no. 11, pp. 3774–3780, 1994.

[16] O. Trepte, "Enhanced scanning control in a confocal scanning laser microscope," *Scanning*, vol. 18, pp. 356–361, 1996.

[17] H. W. Yoo, S. Ito, M. Verhaegen, and G. Schitter, "Iterative Learning Control of a Galvanometer Scanner for Fast and Accurate Scanning Laser Microscopy," in *Mechatronics 2012, 17-19 Sep, Linz, Austria*, 2012, pp. 537–543.

[18] J. Wallén, M. Norrlöf, and S. Gunnarsson, "A Framework for analysis of observer-based-ILC," *Asian Journal of Control*, vol. 13, no. 1, pp. 1–12, 2011.

[19] J. Wallén, I. Dressler, A. Robertsson, M. Norrlöf, and S. Gunnarsson, "Observer-based ilc applied to the gantry-tau parallel kinematic robot," in *Proceedings of 18th IFAC World Congress*, Milano, Italy, Aug. 2011, pp. 992–998.

[20] B. A. Francis and W. M. Wonham, "The internal model principle of control theory," *Automatica*, vol. 12, pp. 457–465, 1976.

[21] R. Munnig Schmidt, G. Schitter, and J. van Eijk, *The design of high performance mechatronics: high-tech functionality by multidisciplinary system integration*. Delft University Press, 2011.

[22] D. A. Bristow, M. Tharayil, and A. G. Alleyne, "A survey of iterative learning control: a learning based method for high-performance tracking control," *IEEE Control System Magazine*, vol. 26, no. 3, pp. 96–114, 2006.

[23] Y. Wu, Q. Zou, and C. Su, "A current cycle feedback iterative learning control approach for AFM imaging," *IEEE Trans. on NanoTech.*, vol. 8, no. 4, pp. 515–527, 2009.

[24] M. Norrlöf and S. Gunnarsson, "Time and frequency domain convergence properties in iterative learning control," *International Journal of Control*, vol. 75, no. 14, pp. 1114–1126, 2002.